A model for the OH defect incorporation in kyanite based on polarised IR spectroscopic investigations

Arkadiusz Wieczorek[1], Eugen Libowitzky[1] and *Anton Beran[1]*

Abstract

Kyanite samples from different geological environments contain structural OH defects equivalent to about 0.0003–0.0058 wt.% H_2O. Two main types of IR spectra can be discerned in the region of the OH stretching vibration. One spectral type contains bands at 3386, 3410 and 3440 cm^{-1} with approximately equal intensities. The second, most common type of kyanite spectra is characterised by a dominating band at 3386 cm^{-1} and only weak bands at 3410 and 3440 cm^{-1}. Clearly separated band maxima occur at 3275 and 3260 cm^{-1}. Slightly turbid crystal parts reveal additional OH absorption features in the 3600 cm^{-1} region which can be assigned to OH groups of layer silicates, occurring as submicroscopic mineral inclusions. From the thermal treatment of kyanite samples up to 1000 °C it is evident that in course of heating processes the included hydrous mineral phases act as hydrogen source for the formation of OH defects inherent to the kyanite structure.

The pleochroic scheme of the 3386 cm^{-1} band, determined on two oriented crystal sections, indicates a preferred orientation of the OH dipole in the n'_β direction of the (100) cleavage plane. This orientation is in coincidence with an incorporation model where O_B acts as donor oxygen of an OH group pointing directly to the centrosymmetric $O_{B'}$ atom. The pleochroic behaviour of the 3440 cm^{-1} band suggests the replacement of O_M oxygen atoms by OH defects roughly pointing to O_C and the pleochroism of the 3410 cm^{-1} band corresponds to a model where O_C acts as donor oxygen of an OH defect roughly pointing to O_M. The pleochroic behaviour of the doublet band at 3275 and 3260 cm^{-1} is in agreement with an OH group where O_F acts as donor and O_A as acceptor oxygen.

Keywords: OH defects, kyanite, IR spectroscopy.

1. Introduction

Nominally anhydrous minerals (NAMs) are known to contain trace amounts of hydrogen, mostly in the form of hydroxyl (OH) groups. The presence of these OH defects can strongly influence the physical and chemical properties of NAMs and the OH concentration may vary as a function of the geological environment and may also be controlled by compositional factors (Libowitzky and Beran, 2004).

Great attention has been devoted to the crystal chemical aspects of the specific modes of trace hydrogen incorporation. The recognition of OH defects in kyanite, Al_2SiO_5, by Beran (1971) was initially based on the observation of infrared (IR) absorption bands in the OH stretching vibrational region of crystals from the classical occurrence of the Alpe Sponda, Switzerland. The presence of OH in kyanites from different localities was confirmed by Wilkins and Sabine (1973). In a detailed IR spectroscopic study based on quantitative data, Beran and Götzinger (1987) established the presence of OH groups in kyanites from different geological environments, including a sample from an eclogite xenolith. OH groups in kyanites from eclogitic mantle xenoliths were also reported by Rossman and Smyth (1990) and by Beran et al. (1993). Kyanite may indeed be a potential storage site for hydrogen in the Earth's upper mantle (Bell and Rossman, 1992; Beran, 1999).

A calibration of the IR spectroscopic data for the water determination in kyanite based on ^{15}N nuclear reaction analysis was presented by Bell et al. (2004), lowering the estimated H_2O values of Beran an Götzinger (1987) by a factor of about 18. OH groups were also identified in the IR spectra of the other alumosilicate polymorphs, andalusite and sillimanite (Beran and Zemann, 1969; Wilkins and Sabine, 1973; Beran et al., 1983, 1989). IR spectroscopy provides an extremely sensitive method for detecting trace hydrogen bonded to oxygen, thus forming OH defects in the structures of various NAMs (Beran and Libowitzky, 2003). Using polarised IR radiation and oriented single-crystal sections, the pleochroic scheme of absorp-

tion bands allows to impose defined constraints on the orientation of the OH dipoles (Libowitzky and Rossman, 1996).

The presence of a band triplet with maxima around 3380, 3405 and 3440 cm^{-1} and of a rather weak but broad band around 3270 cm^{-1} with a satellite absorption at 3260 cm^{-1} were reported for kyanite by Beran and Götzinger (1987). The band around 3380 cm^{-1} was usually the strongest. Approximately equal band intensities of the band triplet are a significant feature of kyanites from eclogite xenoliths (Rossman and Smyth, 1990; Beran et al., 1993). On the basis of the polarisation behaviour of the absorption bands in the 3380 and 3270 cm^{-1} region, Beran (1971) proposed a model for the hydrogen incorporation in the structure of kyanite, with OH groups partially replacing the two crystallographically distinct oxygen atoms which are not bound to silicon atoms. Polarised IR spectra were also reported by Beran et al. (1993) and by Bell et al. (2004) with strong absorptions in the approximate n_α and n_β directions of the optical indicatrix and with only weak absorptions in the n_γ direction.

The aim of this paper is to present a detailed polarised IR spectroscopic study of kyanites with significant OH absorption features, considering also the presence of extrinsic phases such as submicroscopic hydrous inclusions, and to propose a model for the incorporation mode of the intrinsic structural OH defects. Moreover, quantitative information on the concentration range of trace hydrogen in kyanites from different geological environments should be obtained.

2. Experimental

2.1. Samples

Only parts of kyanite single-crystals with excellent optical quality, proved to be optically and spectroscopically free from inclusions and impurities, were used for the detailed polarised measurements to establish the presence of structural OH defects. The microscopic observations were related to an actual total magnification of $400\times$. Slightly turbid samples were used for the IR spectroscopic characterisation of included hydrous mineral phases. Kyanite samples originate from localities in Switzerland, Italy, Russia, South-Africa, Kenya and Tanzania, representing different geological environments and genetic types. The sample characteristics, also referring the IR spectroscopically determined hydrous micro-inclusions, are summarised in Table 1. Some samples show a distinct colour zoning, varying from colourless to dark blue. The FeO contents derived from

Table 1   Localities, occurrence (genetic type), turbidity (hydrous micro-inclusions identified by their OH absorption features), colour of the crystal slabs and water content in wt.%. FeO contents are included under "colour", TiO_2 contents, except for sample 4, and Cr_2O_3 contents, except for sample 5, are lower than 0.1 wt.%; the values are derived from EDX data. IR spectroscopically determined H_2O values were calculated on basis of Beer's law using the integrated molar absorption coefficient $\varepsilon_i = 32900$ l mol^{-1}_{H2O} cm^{-2} (Bell et al., 2004).

No.	Locality	Occurrence	Turbidity	Colour	H_2O content
1	Alpe Sponda Pizzo Forno Switzerland	kyanite-staurolite-qu-fsp nodule in gneiss	mica group minerals (bt + ms)	colourless-blue 0.16	0.0019
2	Dora Maira Italy	pyrope-rutile-kyanite nodule	no OH features	colourless <0.1	0.0041
3	Rangkul, Pamir Russia	isolated crystal	mica group minerals (bt + ms)	colourless-light blue 0.19	0.0016
4	Roberts Victor mine Boshof South-Africa	eclogite xenolith in kimberlite	no OH features	dark blue 0.19 0.13 TiO_2	0.0058
5	Mangari Kenya	tourmaline-ruby-kyanite pegmatite (plumasite)	kaolinite	greenish blue <0.1 0.21 Cr_2O_3	0.0003
6	Kilimanjaro Tanzania	isolated crystal	mica group minerals (bt + ms)	colourless-dark blue <0.1	0.0010

EDX data range up to about 0.2 wt.%, the TiO_2 contents are mostly lower than 0.1 wt.% (Table 1).

Sample preparation consisted of orienting the kyanite single-crystals by morphology and optical methods, followed by preparing two crystal slabs, one slab polished parallel to the (100) cleavage face and a second slab cut perpendicular to (100), parallel to the optical extinction direction of n'_γ. On the (100) slab the polarised IR measurements were related to the n'_β and n'_γ extinction directions. On the second slab the IR measurements were related to the n'_α and n'_γ extinction directions. The two extinction directions in the (100) plane are oriented relatively close to the main n_β and n_γ directions of the indicatrix. The main n_α direction is almost parallel to the *a* lattice parameter. Selected single-crystals were oriented on a CCD single-crystal X-ray diffractometer. Due to the proceeding grinding procedure, the maximum angular deviation of the respective faces from the ideal orientation is estimated to be +/–2°. The indices refer to the lattice parameters $a = 7.126$, $b = 7.852$, $c = 5.572$ Å, $\alpha = 89.99$, $\beta = 101.11$, $\gamma = 106.03°$, space group $P\bar{1}$ (Winter and Ghose, 1979).

2.2. IR spectroscopy

Polarised single-crystal spectra of the oriented kyanite slabs were recorded with a Bruker FTIR spectrometer IFS 66v/S, which was equipped with a Globar light source, a liquid nitrogen-cooled MCT detector and a KRS-5 wire-grid polariser. Background and sample spectra were obtained from 128 scans with a nominal resolution of 2 cm^{-1}. The oriented slabs were mounted on a brass sample holder with a circular aperture of 500 μm in diameter. Absorption figures were obtained after rotation of the sample holder over the range of 180° by steps of 10°. The spectra and the absorption figures are displayed as linear absorption coefficients α in cm^{-1}. The linear absorption coefficient is defined as $\alpha = A/t$, where A is the linear absorbance, $\log(I_0/I)$, and t is the thickness of the crystal slabs measured in cm. Two kyanite samples were thermally treated in a furnace starting at 400 °C in intervals of 100 °C with three hours heating periods, ending up at 1100 °C. After each heating step the samples were cooled down to room temperature within 12 hours.

2.3. Quantitative water determination

The integrated absorbance values A_i (dimension: cm^{-1}) measured parallel to the extinction directions were summed up to get the total integrated absorbance value $A_{i\ total}$ which was used for the calculation of the integrated absorption coefficient α_i (dimension: cm^{-2}), according to the relation $\alpha_i = A_{i\ total} / t$ (sample thickness in cm). As expressed by Beer's law, α_i is directly related by the integrated molar absorption coefficient ε_i (l mol^{-1}_{H2O} cm^{-2}) to the concentration c (mol l^{-1}). The water content in wt.% is calculated using the relationship $c_{H2O} = (1.8/D) (\alpha_i/\varepsilon_i)$, where D is the density of the mineral (in g cm^{-3}) (Beran et al., 1993; Libowitzky and Rossman, 1996; Beran and Libowitzky, 2003). The integrated molar absorption coefficient for OH in kyanite determined by Bell et al. (2004) on the basis of ^{15}N nuclear reaction analysis of hydrogen amounts to 32900 l mol^{-1}_{H2O} cm^{-2} and was used for the calculation of the analytical H_2O values given in Table 1.

In the case of kyanite, the triclinic crystal system renders measurements parallel to extinction directions inconvenient. More convenient approaches have been discussed by Bell et al. (2004) by simply measuring the absorbances parallel to the n'_β extinction direction on the (100) cleavage plane. The calibration of Bell et al. (2004) differs by a factor of about 18 from the calibration of Beran and Götzinger (1987) which was based on the hydrogen determination by a conductometric method. The high water contents determined by Beran and Götzinger (1987) were apparently caused by tiny amounts of submicroscopic hydrous phases – mainly mica group minerals – present in the large amount of sample material (300 mg) that had to be used for the water determination.

It is also worth noting that the molar absorption coefficient $\varepsilon_i = 32900$ l mol^{-1}_{H2O} cm^{-2} determined by Bell et al. (2004) is by a factor of about three lower than that expected from the linear calibration curve given by Libowitzky and Rossman (1997), where the predicted values range around 90000 l mol^{-1}_{H2O} cm^{-2}. Thus, kyanite presents another example, in addition to that of pyrope, rutile, cassiterite and olivine, where the general correlation between integrated molar absorption coefficients and OH band positions does not strictly hold (Libowitzky and Rossman, 1997; Maldener et al., 2001; Bell et al., 2003; Losos and Beran, 2004).

3. Results

Polarised OH absorption spectra of selected kyanite samples measured on (100) plates with the electric vector of the polarised IR radiation vibrating parallel to the n'_β extinction direction are shown in Fig. 1. Dominant absorption bands occur in the 3700–3200 cm^{-1} region. Two main spectral types can be discerned. One type is represented

by the sample from the Roberts Victor mine, consisting of a band triplet with individual bands at 3386, 3410 and 3440 cm⁻¹ of approximately equal intensities. This homogeneously dark blue kyanite occurs in eclogitic mantle xenoliths and has significantly enhanced values of Ti (0.13 wt.% TiO_2). The low-energy bands are relatively broad and show one single maximum around 3275 cm⁻¹.
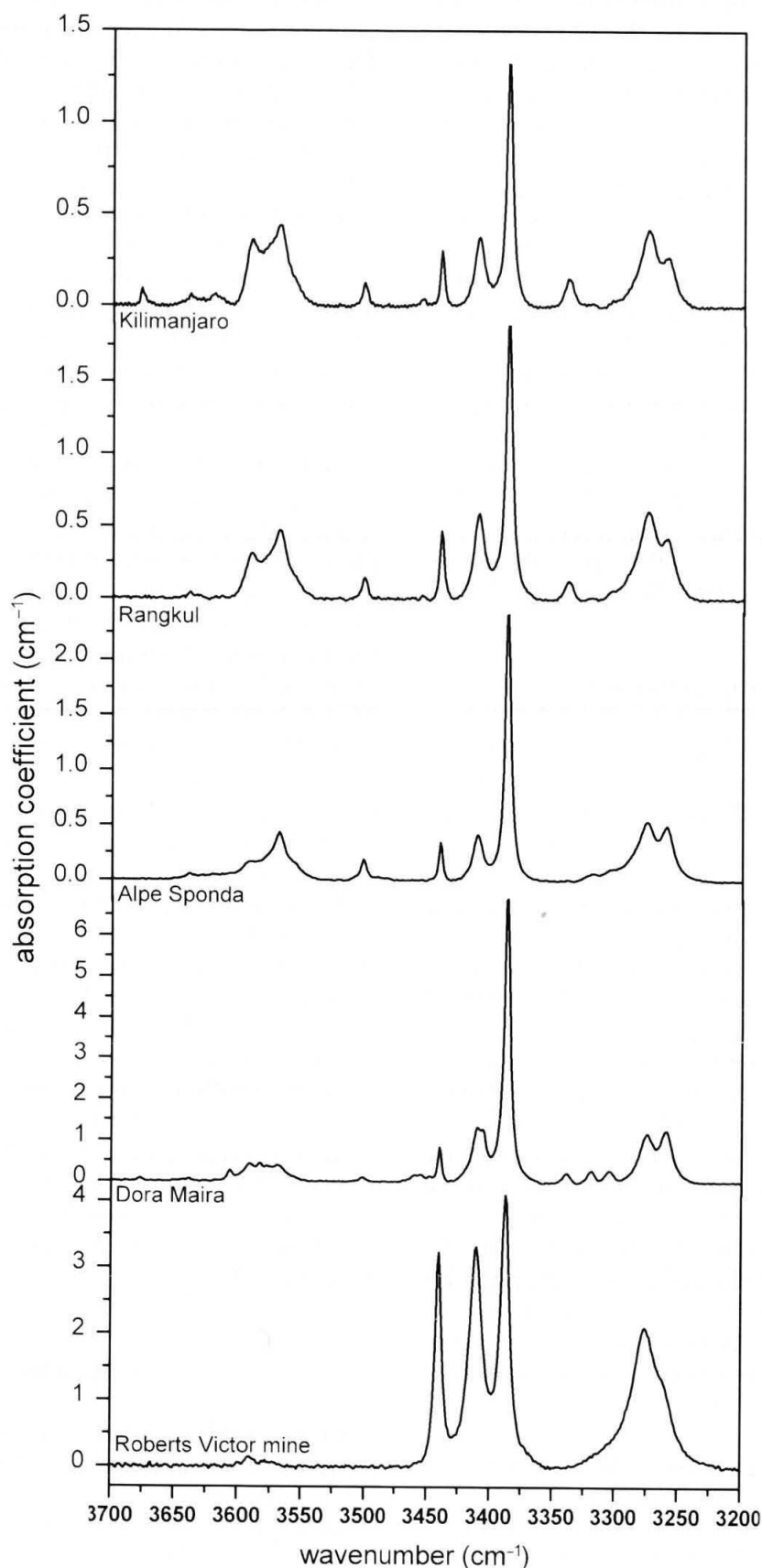

Fig. 1 Polarised OH absorption spectra of kyanites measured on (100) slabs parallel to the n'$_\beta$ extinction direction. Note the different scales of absorption coefficients.
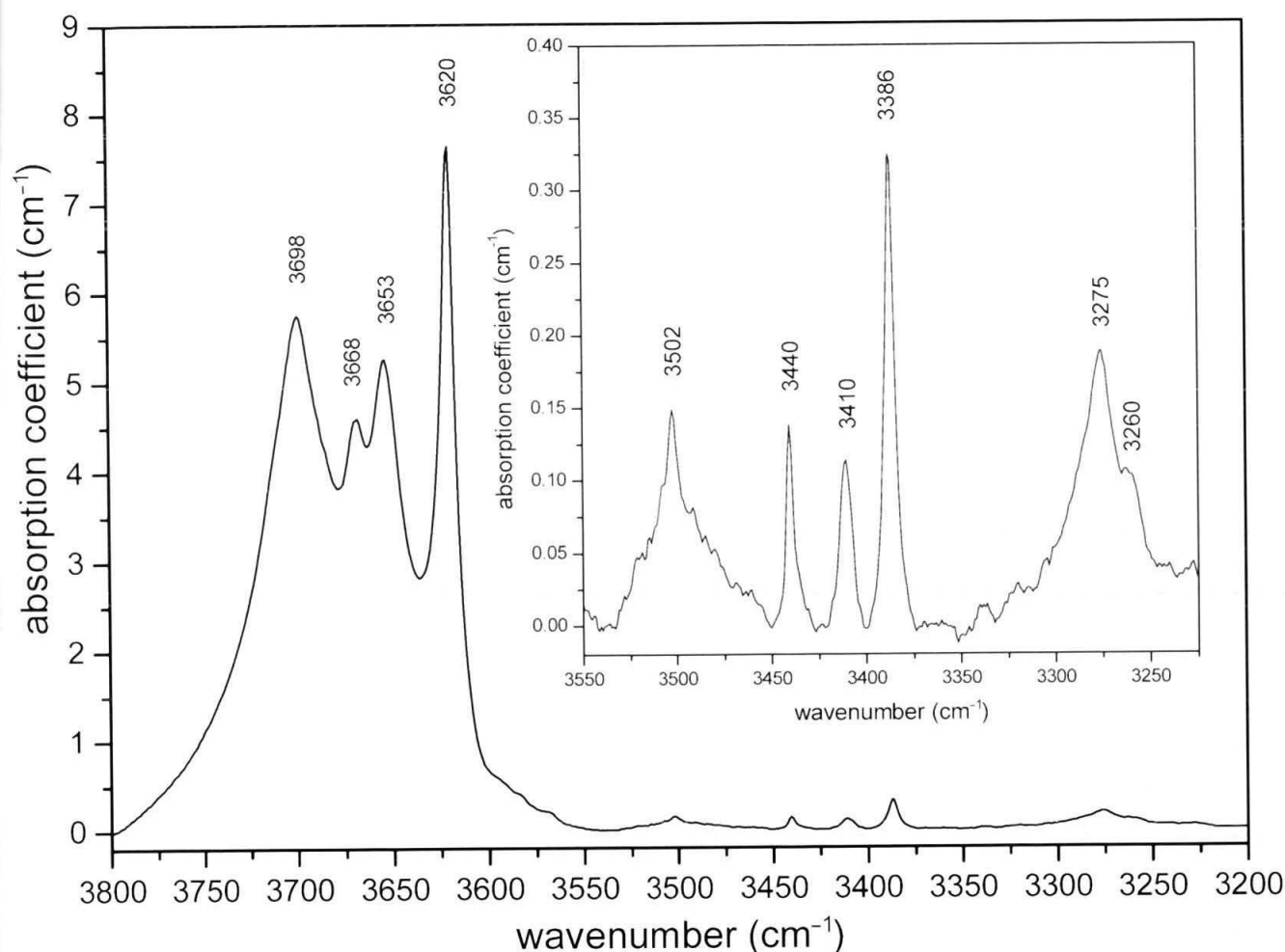
Fig. 2 Unpolarised IR spectrum in the OH stretching vibrational range of kyanite from Mangari, taken through turbid crystal parts. The strong OH absorption features in the 3600–3750 cm^{-1} region correspond to those of kaolinite. The OH bands of the kyanite host are shown in the inset.

Band deconvolution revealed a satellite band at 3260 cm^{-1}. An additional maximum at 3295 cm^{-1} can be discerned by band deconvolution only in the n$'_\alpha$ spectrum of this sample. OH spectra of kyanites from mantle rocks reported in the literature (Rossman and Smyth, 1990; Beran et al., 1993; Bell et al., 2004) show similar features and can also be attributed to this spectral type. The most common and frequently occurring type of kyanite spectra is represented by the spectra of the samples from Dora Maira and Alpe Sponda showing a dominating single band at 3386 cm^{-1} and only very low intensities of the bands at 3410 and 3440 cm^{-1}. Especially the Dora Maira sample is characterised by a separation of the 3410 cm^{-1} band, leading to an additional maximum at 3405 cm^{-1}. The spectra of the samples from Rangkul and Kilimanjaro can be named as "intermediate" and are characterised by somewhat higher intensities of the 3410 and 3440 cm^{-1} bands. The band maxima at 3275 and 3260 cm^{-1} are clearly separated and show comparable intensities (Fig. 1). In colour-zoned crystals, varying from colourless to

dark blue, only the colourless and light blue crystal parts reveal OH absorption bands, whereas the dark blue parts show no OH absorption features in this energy region at all.

As evidently seen in the spectra of Fig. 1, additional absorption features occur in the high-energy OH stretching vibrational region around 3600 cm^{-1}. These absorptions can be assigned to OH groups of layer silicates (Farmer, 1974; Beran, 2002), occurring as submicroscopic mineral inclusions. Spectral features of muscovite, biotite and kaolinite are most commonly encountered (Table 1). The observed pleochroic behaviour of these bands suggests an oriented intergrowth. As shown in Fig. 2, the characteristic absorptions of kaolinite with maxima at 3620, 3653, 3668 and 3698 cm^{-1} (Farmer, 1974) clearly confirm the source of turbidity in kyanites from Mangari, also demonstrating that IR spectroscopy is a useful method for the identification and characterisation of very small amounts of fine-grained contaminating hydrous mineral phases which cannot be identified under a polarising microscope with 400× to-
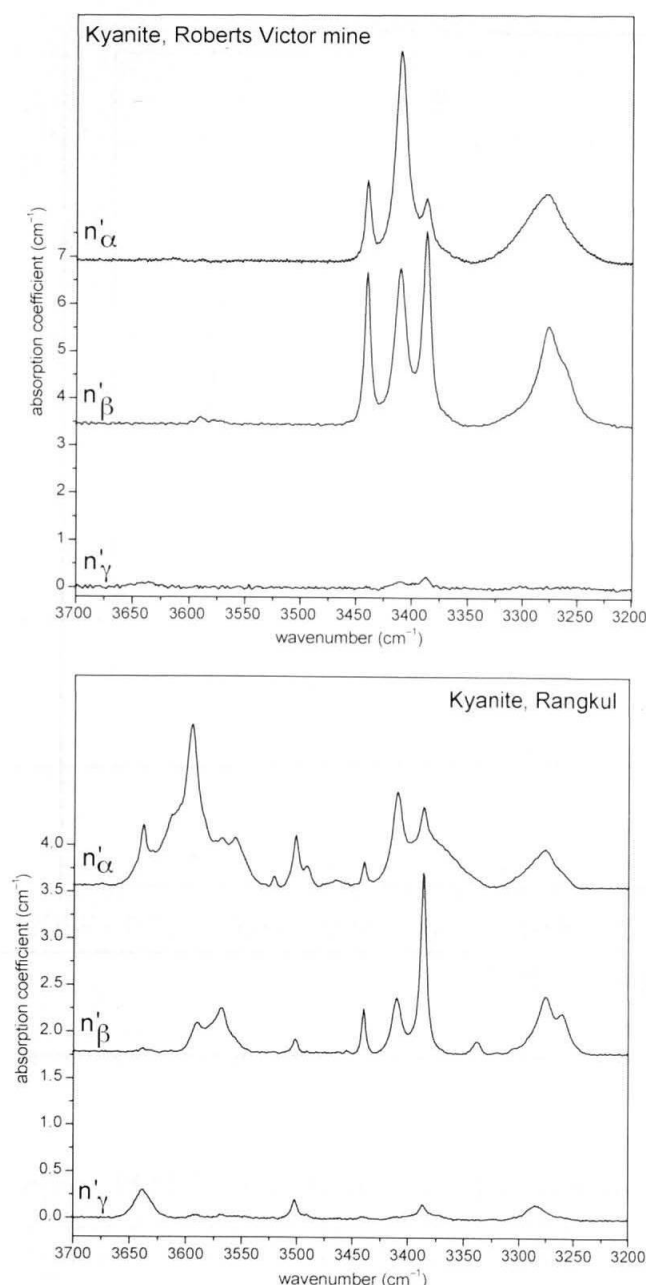
Fig. 3 Polarised OH absorption spectra of kyanites from Roberts Victor mine and Rangkul, recorded parallel to the n'_α, n'_β and n'_γ extinction directions on (100) crystal plates and on plates cut parallel to n'_γ and perpendicular to (100). Spectra are offset for clarity. The strong bands above 3500 cm^{-1} in the sample from Rangkul are caused by submicroscopic hydrous mineral inclusions.

tal magnification. However, the presence of additional anhydrous mineral phases contributing to the turbidity of the crystals cannot be ruled out.

As a significant feature of all kyanites the high-energy band triplet with bands centred at 3386, 3410 and 3440 cm^{-1} and the low-energy band doublet with bands at 3260 and 3275 cm^{-1} show maximum absorption in (100) when the vector E of the polarised radiation vibrates parallel to the n'_β extinction direction. In the plane cut parallel to

n'_γ and perpendicular to (100) maximum absorption for these bands occurs when the E vector vibrates parallel to n'_α. Only weak absorption components are observed in the n'_γ direction, resulting in a strong pleochroism in both crystal plates. The polarised IR absorption spectra of the samples from Rangkul and from Roberts Victor mine measured parallel to the n'_α, n'_β and n'_γ directions are shown in Fig. 3, also demonstrating the pleochroism of the OH bands attributed to oriented hydrous mineral inclusions. For the kyanite sample from Rangkul, as a typical example, the corresponding OH absorption figures for the intrinsic structural OH defects are presented in Fig. 4, demonstrating the coincidence of the absorption maxima and minima with the optical extinction directions. Observations of changes of band intensities are based on the deconvolution of the spectra into single Gaussian- and Lorentzian-shaped component bands provided by the program PeakFit (Jandel Scientific). As an example, the baseline-corrected and deconvoluted n'_β spectrum of the kyanite sample from Rangkul is shown in Fig. 5.

Heating experiments performed on (100) cleavage slabs of kyanites from Rangkul, containing small amounts of hydrous mineral inclusions and of pure kyanites from Roberts Victor mine, containing no spectroscopically detectable inclusions, clearly indicate hydrogen diffusion processes (Fig. 6). In the pure kyanite up to 500 °C the intensity of the band at 3386 cm^{-1} slightly increases whereas the intensities of the neighbouring bands at 3410 and 3440 cm^{-1} show a significant decrease. A slight decrease in the intensities of all three bands starts at 700 °C and continues with an abrupt decrease at 900 °C. Further heating to 1000 °C causes all bands to disappear. Up to 800 °C the intensities of the low-energy band group at 3260 and 3275 cm^{-1} remain nearly constant followed by a strong decrease and vanishing of the bands at 1000 °C. A different heating behaviour at high temperatures is evident for the Rangkul sample, containing hydrous mineral inclusions (Fig. 3). A significant increase of the band intensities of the band triplet and of the low-energy band doublet between 700 and 900 °C is clearly related to the loss of intensity of OH bands which are due to the presence of included hydrous phases, probably mainly biotite. Most of the water is released at 1000 °C, no OH of the hydrous inclusions and only extremely small amounts of structural OH defects are detectable after annealing at 1000 °C. It is evident that in course of the heating processes the included hydrous mineral phases act as internal hydrogen source for the formation of additional structural OH defects.

4. Discussion

The triclinic crystal structure of kyanite, Al_2SiO_5, can be described on the basis of a distorted close-packed oxygen arrangement. The aluminum cations fill 40% of the octahedral interstices in such a way that half of the occupied octahedra form single chains parallel to the c-axis. The silicon atoms occupy 10% of the tetrahedrally coordinated structural sites. There are two crystallographically distinct silicon (Si_1 and Si_2), four aluminum (Al_1, Al_2, Al_3 and Al_4) and ten oxygen atoms (O_A, O_B, O_C, O_D, O_E, O_F, O_G, O_H, O_K and O_M) in the unit cell (Burnham, 1963; Winter and Ghose, 1979). Eight oxygen atoms are coordinated by one Si and two Al, forming the top of a flat distorted trigonal pyramid. Two oxygen atoms (O_B and O_F), not bound to Si, are coordinated by four Al.

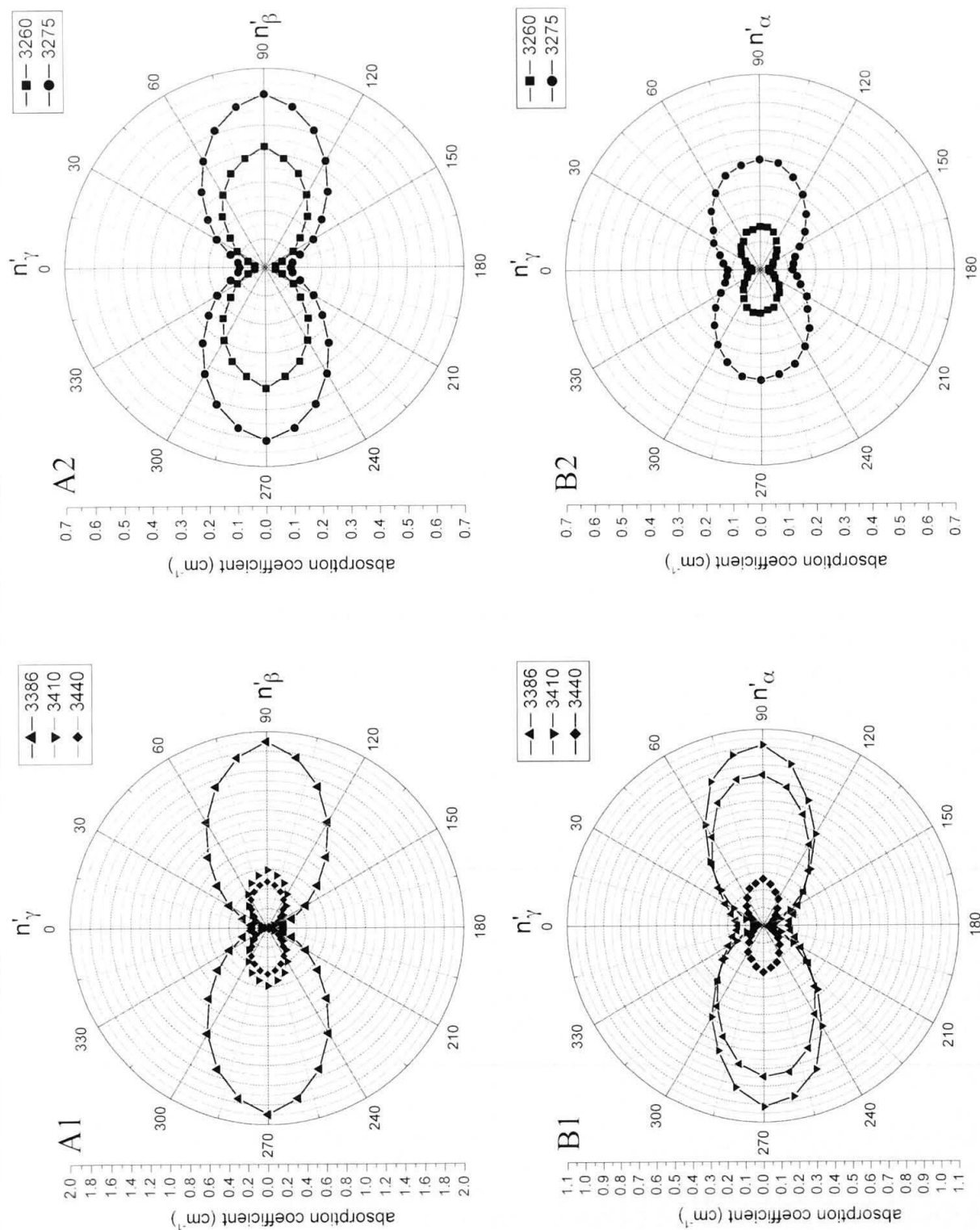The pleochroic scheme of the OH absorption bands imposes certain constraints on the orienta-

Fig. 4 OH absorption figures for the bands at 3386, 3410, 3440 cm^{-1} and 3260, 3275 cm^{-1} of kyanite from Rangkul: A1 and A2 show the measurements on a (100) plate related to the n'_β and n'_γ extinction directions; B1 and B2 show the measurements on a plate cut parallel to n'_γ and perpendicular to (100) related to the n'_α and n'_γ extinction directions.
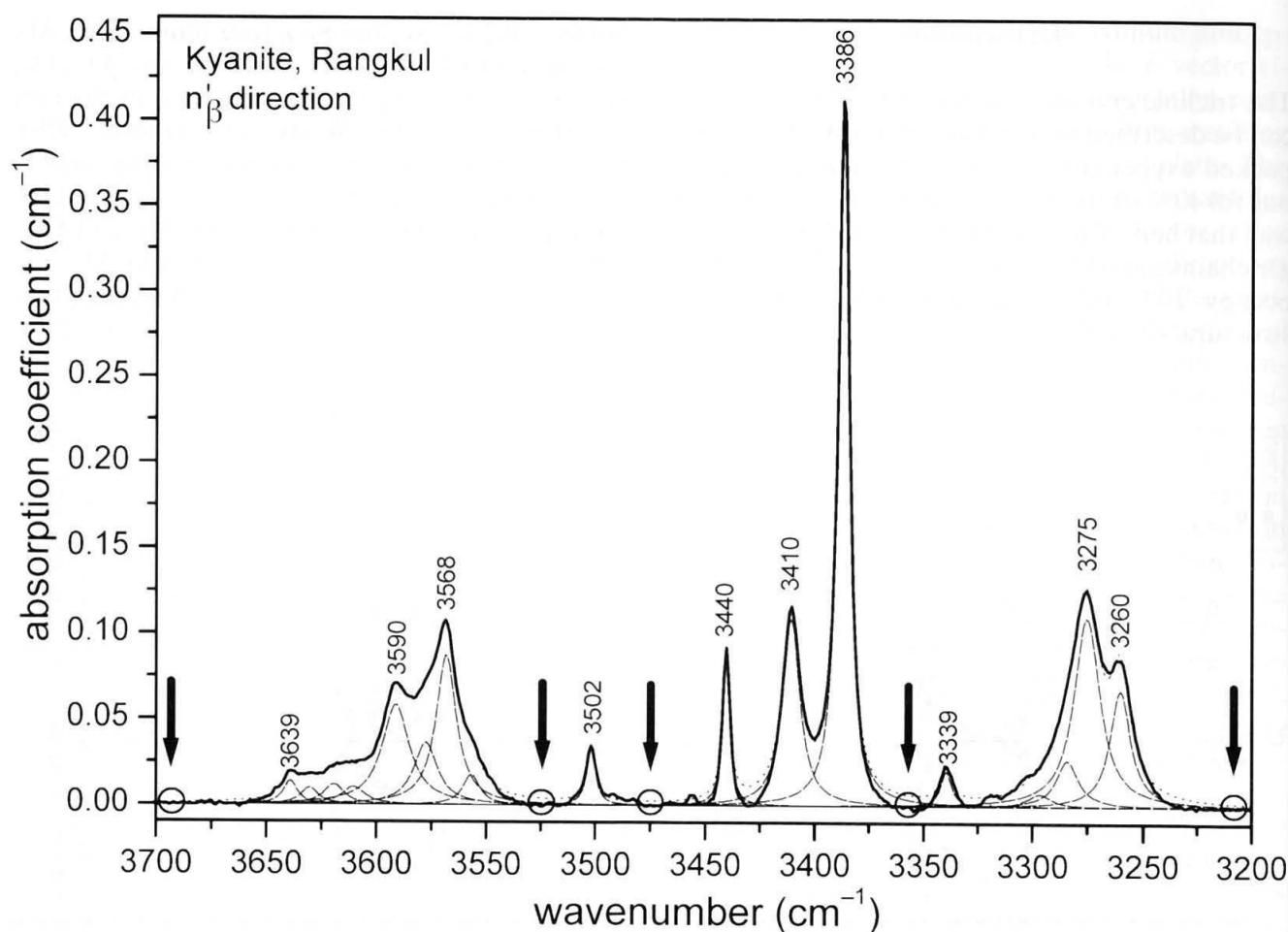
Fig. 5 Polarised OH absorption spectrum of kyanite from Rangkul subjected to a band deconvolution procedure by the program PeakFit. Five reference points (indicated by black arrows) were used for constraining the background position of the individual spectra.

tion of the OH dipoles. The extremely strong pleochroism of the band triplet at 3386, 3410 and 3440 cm^{-1} and the band doublet at 3260 and 3275 cm^{-1} with strong absorptions parallel to n'_α and n'_β and only a weak absorption component parallel to n'_γ requires an alignment of the OH vector directions within the plane formed by n'_α and n'_β. The band at 3386 cm^{-1} shows the most distinct difference in the absorption components within this plane, demanding a preferred orientation of the OH dipole in the n'_β direction. This orientation is in coincidence with an incorporation model where O_B acts as donor oxygen of an OH group directly pointing to the centrosymmetric $O_{B'}$ atom. The O_B oxygen is coordinated by four Al and not bound to Si (Fig. 7 a). Also the band at 3440 cm^{-1} shows a distinct but less pronounced difference in the absorption components parallel to n'_α and n'_β. This direction is in agreement with the replacement of an O_M oxygen atom by an OH defect roughly pointing to the O_C oxygen atom. Considering the pleochroic behaviour of the 3410 cm^{-1} band showing a stronger absorption component parallel to n'_α, a model is developed where

O_C acts as donor oxygen of an OH defect roughly pointing to O_M, now acting as acceptor oxygen of a very weak bent hydrogen bond. The difference in the directions of the OH dipoles, O_M-H···O_C and O_C-H···O_M, is related to the different positions of the plane formed by the three coordinating cations (2 Al + 1 Si), representing a positively charged electrostatic field. Usually OH dipole directions are oriented approximately perpendicular to the coordinating cation plane.

The low-energy doublet band at 3275 and 3260 cm^{-1} shows a uniform pleochroic behaviour with a slightly stronger absorption component parallel to n'_β. The weak pleochroism within the n'_α–n'_β plane is in agreement with an OH dipole direction where O_F acts as donor and O_A as acceptor oxygen (Fig. 7b). The distinct splitting of this band can be explained by the substitution of one of the coordinating cations, e.g. the replacement of one Al by one Fe. A minor substitution of the two oxygen atoms which are not bound to Si, i.e. O_F and O_B, was originally proposed by Beran (1971). A separated absorption band at 3295 cm^{-1} can be observed after band deconvolution in the n'_α spec-
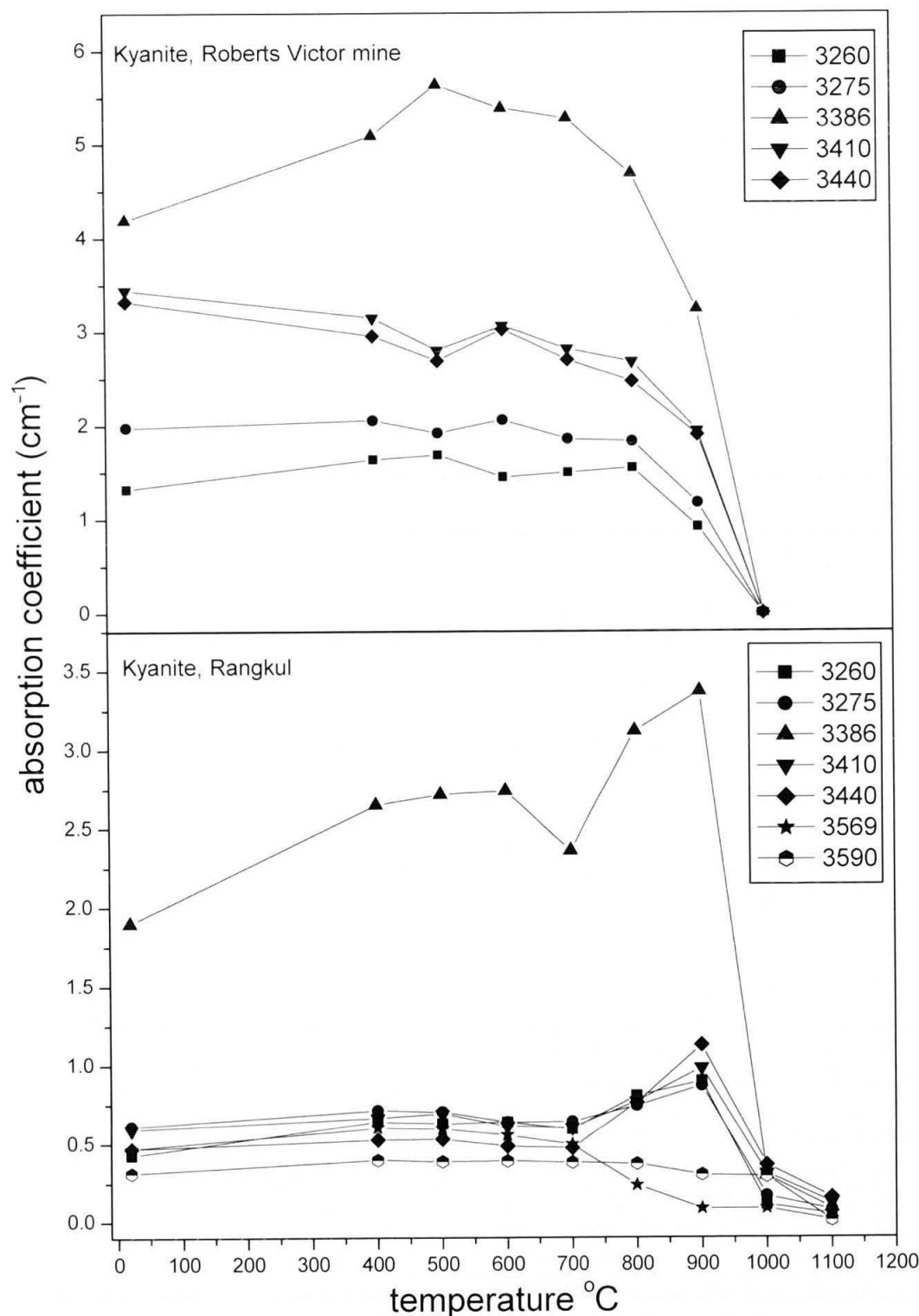
Fig. 6 Dehydration curves, i.e. intensities of various absorption bands versus temperature (heating periods of three hours), of pure kyanite from Roberts Victor mine and of kyanite from Rangkul containing submicroscopic inclusions of hydrous mineral phases.

trum of kyanite from Roberts Victor mine indicating an OH orientation parallel to n'_α. A partial replacement of the O_H oxygen atom by OH groups pointing to a centrosymmetric $O_{H'}$ atom seems to be the most likely interpretation. The extremely small splitting of the 3410 cm^{-1} band creating an additional band maximum at 3405 cm^{-1} in the Dora Maira sample, can be explained by the replace-

ment of Al by Fe in the coordination triangle of the O_M atom, forming the acceptor oxygen of the O_C-H$\cdots O_M$ bond. Due to the low Fe concentrations, these models would require a strong short-range ordering of OH and Fe. No other plausible OH incorporation models can be developed considering O-H$\cdots$O directions which are in rough agreement with the measured pleochroic scheme.
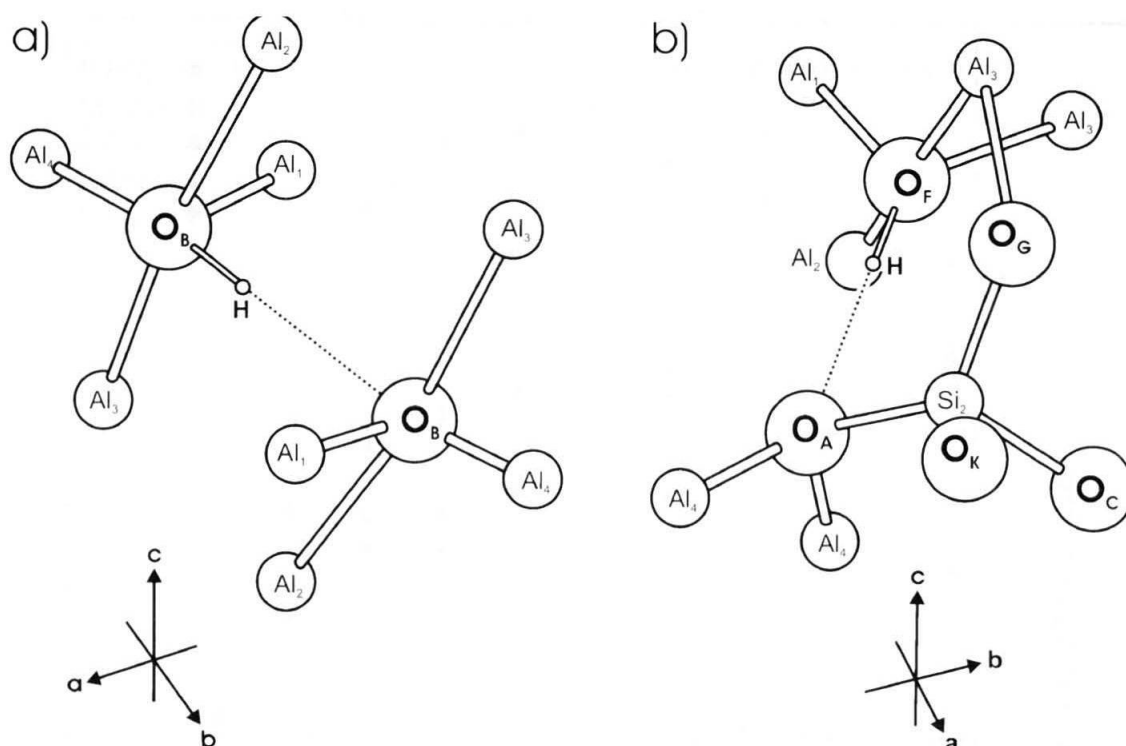
Fig. 7 Part of the kyanite crystal structure demonstrating the proposed OH defect incorporation model for (a) partial OH replacement of the O_B oxygen position, related to the band at 3386 cm⁻¹, (b) partial OH replacement of the O_F oxygen position, related to the doublet band at 3275 and 3260 cm⁻¹.

Empirical correlation diagrams of OH stretching frequencies versus O-H···O distances as presented by Novak (1974) and especially for minerals by Libowitzky (1999) cannot directly be applied to the present OH defect model discussed on the basis of the ideal kyanite structure. The low wavenumbers of the absorption bands related to the proposed OH defect positions are not in agreement with the relatively large O-H···O distances which are derived from the structure and consequently lead to the assumption of local structural distortions. However, the relative positions of the bands are in agreement with these general correlations. In the ideal structure the O_B-$O_{B'}$ distance amounts to 3.39 Å and the O_F-O_A distance to 3.14 Å. In both cases a straight hydrogen bond can be expected and the distances correlate with the bands at 3386 cm⁻¹ and 3275/3260 cm⁻¹, respectively. The relatively short O_C-O_M, respectively O_M-O_C distance of about 3.03 Å is not in contradiction to this correlation, as we have to expect strongly bent hydrogen bonds for the defects related to the bands at 3410 and 3440 cm⁻¹.

As evident from Fig. 1 the band at 3386 cm⁻¹ is most prominent in all kyanite samples. On the basis of the proposed model, the O_B site presents the preferred position for the OH defect incorporation in the structure of kyanite, assuming a complete occupancy of the cation positions. As shown in Table 1, the water content varies from 0.0003 to

0.0058 wt.% suggesting different water activities prevalent in the corresponding geological environment. One may speculate, whether high water contents are related to kyanites formed under high P–T conditions.

Acknowledgements

References

Bell, D.R. and Rossman, G.R. (1992): Water in Earth's mantle: The role of nominally anhydrous minerals. *Science* **255**, 1391–1397.
Bell, D.R., Rossman, G.R., Maldener, J., Endisch, D. and Rauch, F. (2003): Hydroxide in olivine: A quantitative determination of the absolute amount and calibration of the IR spectrum. *J. Geophys. Res.* **108/B2**, 2105–2113.
Bell, D.R., Rossman, G.R., Maldener, J., Endisch, D. and Rauch, F. (2004): Hydroxide in kyanite: A quantitative determination of the absolute amount and calibration of the IR spectrum. *Am. Mineral.* **89**, 998–1003.
Beran, A. (1971): Messung des Ultrarot-Pleochroismus von Mineralen XII. Der Pleochroismus der OH-Streckfrequenz in Disthen. *Tschermaks Min. Petr. Mitt.* **16**, 129–135.

Beran, A. (1999): Contribution of IR spectroscopy to the problem of water in the Earth's mantle. In: Wright, K. and Catlow, R. (eds.): Microscopic properties and processes in minerals. Kluwer Acad. Publ., Dordrecht, 523–538.

Beran, A. (2002): Infrared spectroscopy of micas. In: Mottana, A. et al. (eds.): Micas: Crystal chemistry and metamorphic petrology. *Rev. Mineral. Geochem.* **46**, Mineral. Soc. Am., / Accad. Nat. Lincei, Roma, 351–369.

Beran, A. and Götzinger, M.A. (1987): The quantitative IR spectroscopic determination of structural OH groups in kyanites. *Mineral. Petrol.* **36**, 41–49.

Beran, A. and Libowitzky, E. (2003): IR spectroscopic characterization of OH defects in mineral phases. *Phase Trans.* **76**, 1–15.

Beran, A. and Zemann, J. (1969): Messung des Ultrarot-Pleochroismus von Mineralen VIII. Der Pleochroismus der OH-Streckfrequenz in Andalusit. *Tschermaks Min. Petr. Mitt.* **13**, 285–292.

Beran, A., Hafner, S. and Zemann, J. (1983): Untersuchungen über den Einbau von Hydroxilgruppen im Edelstein-Sillimanit. *N. Jb. Mineral., Mh.* **1983**, 219–226.

Beran, A., Langer, K. and Andrut, M. (1993): Single crystal infrared spectra in the range of OH fundamentals of paragenetic garnet, omphacite and kyanite in an eclogitic mantle xenolith. *Mineral. Petrol.* **48**, 257–268.

Beran, A., Rossman, G.R. and Grew, E. (1989): The hydrous component of sillimanite. *Am. Mineral.* **74**, 812–817.

Burnham, C.W. (1963): Refinement of the crystal structure of kyanite. *Z. Kristallogr.* **118**, 337–360.

Farmer, V.C. (1974): The layer silicates. In: Farmer, V.C. (ed.): The infrared spectra of minerals. Mineral. Soc., London, 331–363.

Libowitzky, E. (1999): Correlation of O–H stretching frequencies and O–H···O hydrogen bond lengths in minerals. *Mh. Chem.* **130**, 1047–1059.

Libowitzky, E. and Beran, A. (2004): IR spectroscopic characterisation of hydrous species in minerals. In: Beran, A. and Libowitzky, E. (eds.): Spectroscopic Methods in Mineralogy. *EMU Notes in Mineralogy* **6**, Eur. Min. Union / Eötvös University Press, Budapest, 227–279.

Libowitzky, E. and Rossman, G.R. (1996): Principles of quantitative absorbance measurements in anisotropic crystals. *Phys. Chem. Minerals* **23**, 319–327.

Libowitzky, E. and Rossman, G.R. (1997): An IR absorption calibration for water in minerals. *Am. Mineral.* **82**, 1111–1115.

Losos, Z. and Beran, A. (2004): OH defects in cassiterite. *Mineral. Petrol.* **81**, 219–234.

Maldener, J., Rauch, F., Gavranic, M. and Beran, A. (2001): OH absorption coefficients of rutile and cassiterite deduced from nuclear reaction analysis and FTIR spectroscopy. *Mineral. Petrol.* **71**, 21–29.

Novak, A. (1974): Hydrogen bonding in solids. Correlation of spectroscopic and crystallographic data. *Struct. Bond.* **18**, 177–216.

Rossman, G.R. and Smyth, J.R. (1990): Hydroxyl contents of accessory minerals in mantle eclogites and related rocks. *Am. Mineral.* **75**, 775–780.

Wilkins, R.W.T. and Sabine, W. (1973): Water content of some nominally anhydrous silicates. *Am. Mineral.* **58**, 508–516.

Winter, J.K. and Ghose, S. (1979): Thermal expansion and high-temperature crystal chemistry of the Al_2SiO_5 polymorphs. *Am. Mineral.* **64**, 573–586.